



Sentinel-3 Delay-Doppler Altimetry over Antarctica

Malcolm McMillan¹, Alan Muir², Andrew Shepherd¹, Roger Escolà³, Mònica Roca³, Jérémie Aublanc⁴,
Pierre Thibaut⁴, Marco Restano⁵, Américo Ambrozio⁵, Jérôme Benveniste⁵

5

¹Centre for Polar Observation & Modelling, University of Leeds, Leeds, LS2 9JT, UK

²University College London, Gower Street, London, WC1E 6BT, UK

³IsardSAT Ltd, Surrey Space Incubator, 40 Occam Road, The Surrey Research Park, Guildford, Surrey GU2 7YG, UK

⁴CLS, 11 Rue Hermes, Parc Technologique du Canal, 31520 Ramonville Saint-Agne, France

10 ⁵ESA ESRI, Largo Galileo Galilei, 1, 00044 Frascati RM, Italy

Correspondence to: Malcolm McMillan (m.mcmillan@leeds.ac.uk)

Abstract. On 16th February 2016, the launch of the Sentinel-3A satellite marked the first step towards a new era of operational Delay-Doppler altimetry over ice sheets. Given the provision of these novel altimeters for decades to come, and
15 the long-term benefits they can offer to a range of glaciological applications, it is important to establish their capacity to monitor ice sheet elevation and elevation change. Here, we present the first analysis of Sentinel-3 Delay-Doppler altimetry over the Antarctic Ice Sheet, and assess the accuracy and precision of retrievals of ice sheet elevation across a range of topographic regimes. Over the ice sheet interior, we find that the instrument achieves both an accuracy and a precision of the order of 10 cm, with ~98% of the data validated being within 50 cm of co-located airborne measurements. Across coastal
20 regions, which exhibit steeper and more complex topography, the accuracy decreases slightly, although ~60-85% of validated data are still within 1 meter of co-located airborne elevation measurements. Finally, we explore the utility of the instrument for mapping elevation change, and show that, with less than 2 years of available data, it is possible to resolve known signals of ice dynamic imbalance. Our analysis demonstrates a new, long-term source of measurements of ice sheet elevation and elevation change, and the early potential of this novel operational system for monitoring ice sheet imbalance
25 for decades to come.



1. Introduction

Accurate knowledge of ice sheet topography and regional changes in ice volume are essential for developing a process-based understanding of ice sheet evolution, and for monitoring the response of Greenland and Antarctica to climate change [Shepherd *et al.*, 2004; Davis *et al.*, 2005; Price *et al.*, 2011]. For the past quarter of a century, satellite radar altimeters have provided near-continuous coverage of Earth's Polar regions, yielding detailed topographic information of ice sheets [Remy *et al.*, 1989; Bamber and Bindschadler, 1997; Bamber *et al.*, 2009; Helm *et al.*, 2014], together with estimates of changes in ice sheet volume [Davis and Ferguson, 2004; Johannessen *et al.*, 2005; Helm *et al.*, 2014] and mass [Wingham *et al.*, 2006b; Zwally *et al.*, 2011; Shepherd *et al.*, 2012; McMillan *et al.*, 2014, 2016]. By resolving changes at the scale of individual glacier basins, these satellites have been able to identify emerging signals of imbalance [Wingham *et al.*, 2009; Flament and Rémy, 2012], loci of rapid ice loss [Zwally *et al.*, 2005; Hurkmans *et al.*, 2014; Sørensen *et al.*, 2015; McMillan *et al.*, 2016], and the regional contribution of ice sheets to global sea level rise [Zwally *et al.*, 2011; Shepherd *et al.*, 2012].

During the earlier part of this 25-year record, missions carried conventional low resolution, or *pulse-limited*, instruments, including those flown onboard the ERS-1, ERS-2, Envisat and SARAL satellites. These systems, which were originally developed to measure the ocean geoid, flew to a latitude of $\sim 81^\circ$, and provided a ground footprint of approximately 2 km^2 (Ku-band pulse-limited footprint over a flat, orthogonal surface). The size of this footprint, together with the large area illuminated by the radar antenna beam ($\sim 200 \text{ km}^2$), meant that correctly locating the origin of the surface reflection in regions of complex terrain was challenging. In 2010, the first dedicated ice radar altimetry mission, CryoSat-2, was launched, with two improvements in system design that were specifically aimed at enhancing altimeter performance in areas of steep and complex ice margin terrain. Synthetic Aperture Radar (SAR), or *Delay-Doppler*, processing delivered a four-fold improvement in along-track resolution, to approximately 400 m, and interferometric techniques were used to locate the origin of the surface reflection in the across-track plane [Raney, 1998; Wingham *et al.*, 2006a]. These developments, in conjunction with the unique long-period, high-inclination orbit, have delivered improved coverage of Earth's ice sheets [McMillan *et al.*, 2014, 2017], and yielded greater confidence in determining their ongoing evolution.

With CryoSat-2 now operating far beyond its original design lifetime of 3.5 years, and a new era of Copernicus operational Delay-Doppler altimetry missions commencing, there is presently a need to establish the utility of the new class of Sentinel-3 radar altimeter satellites [Donlon *et al.*, 2014] for the purpose of monitoring ice sheet change. The first of four satellites, Sentinel-3A, was launched on 16th February 2016, and was followed by Sentinel-3B on 25th April 2018. Each satellite provides coverage up to a latitude of 81.35° , with 385 orbital revolutions per cycle, yielding an on-the-ground revisit time of 27 days (Table 1), together with a 4-day sub-cycle. The main altimetry payload, *SRAL*, is a Ku-band SAR altimeter, which provides elevation measurements with a resolution of $\sim 300 \text{ m}$ along-track by $\sim 1.6 - 3 \text{ km}$ across-track, depending upon the surface roughness [Chelton *et al.*, 1989]. To date, the focus of Sentinel-3 exploitation has been upon retrievals over ocean



and inland water surfaces, with early studies demonstrating the novel capability to retrieve fine-scale (~20 km) oceanographic features [Heslop *et al.*, 2017], to increase the quality of river level and discharge estimates in Central Africa [Bogning *et al.*, 2018] and to resolve near-coastal sea surface height [Bonnefond *et al.*, 2018].

- 5 Over ice sheet surfaces, Sentinel-3 is unique among altimeters, because it operates in Delay-Doppler mode across all regions. This mode of operation contrasts with CryoSat-2, which operates in Low Resolution Mode over the interior of each ice sheet and SAR interferometric mode at coastal locations. As a consequence, although no interferometric information is available to aid Sentinel-3 retrievals around the ice sheet margins, high resolution measurements are for the first time routinely acquired throughout the ice sheet interior. Given the novelty of the Sentinel-3 instrument across both inland and coastal ice sheet
- 10 regions, together with the future longevity of the EU Copernicus programme of operational satellites, it is imperative that early assessments of the accuracy and precision of the instrument are made over ice sheet surfaces, to establish the basis for glaciological applications of these data. Here we provide a first evaluation of Sentinel-3 Delay-Doppler measurements over Antarctica, to determine its utility for monitoring ice sheet surfaces.

15 2. Study Sites

- To evaluate Sentinel-3 Delay-Doppler altimeter performance across a range of topographic regimes, we selected four study sites across Antarctica (Figure 1). Two sites – the areas surrounding Lake Vostok and Dome C – are located within the interior of the East Antarctic Ice Sheet and are characterized by relatively simple topography. These sites allowed us to evaluate the performance of Delay-Doppler altimetry in regions representative of a large part of the Antarctic interior. Both
- 20 sites have low and relatively uniform topographic slopes, with an average and standard deviation of 0.09° and 0.05° (Lake Vostok), and 0.04° and 0.03° (Dome C), respectively, based upon a 1km Digital Elevation Model (DEM) [Slater *et al.*, 2017]. Furthermore, the flat ice surface directly above Lake Vostok represents an established validation site for novel altimetry missions [Shuman *et al.*, 2006; Richter *et al.*, 2014; Schröder *et al.*, 2017]. To assess performance in regions of steeper and more complex topography, we also selected two coastal sites covering parts of Dronning Maud Land and Wilkes
- 25 Land (Figure 1). These locations were chosen because of the availability of airborne campaigns that could be used as independent validation. Both sites have an order of magnitude steeper and less uniform topography than the inland sites, with the mean and standard deviation of the surface slope being 0.50° and 0.94° (Dronning Maud Land) and 0.40° and 0.51° (Wilkes Land), respectively.



3. Altimeter Data & Processing Methods

We analyzed 24 cycles of Sentinel-3A SRAL data acquired between December 2016 and December 2017. Our processing followed a standard chain, starting with the 20 Hz waveform data provided by the European Space Agency (ESA) within their freely-distributed ‘enhanced’ data file, and generated using their Processing Baseline 2.27. First, unusable waveforms, where no clear leading edge could be identified, were rejected and not passed to the subsequent processing. Then, each remaining waveform was retracked using a variety of empirical retrackers, including a Threshold on the offset Centre of Gravity amplitude (TCOG) [Wingham *et al.*, 1986], a Threshold First Maximum Retracker (TFMRA) [Helm *et al.*, 2014], and a maximum gradient of the first leading edge retracker [Gray *et al.*, 2015]. For the first two solutions, a threshold of 50 % of the waveform power was selected, with the aim of providing a stable retracking point across both low slope and more complex topographic surfaces. More specifically, we chose this mid-power threshold as a balance between minimising the sensitivity to noise at the start of the waveform leading edge, and also to reducing the impact radar speckle, which is more apparent near the waveform peak due to its multiplicative nature. For the majority of this study, we focused on results produced by the TCOG retracking, because of the continuity it provides with the ground segments of past European Space Agency (ESA) missions, and the broadly consistent results between all three of the retrackers tested.

After retracking, Level-2 instrument and geophysical corrections were applied to each range measurement to account for the distance between the antenna and satellite centre of mass, dry and wet troposphere delays, ionosphere delays, solid Earth tide, ocean loading tide and Polar tide, plus ocean tide and the inverse barometer effect over floating ice. These corrections are all included within the enhanced data product, although the geophysical corrections are provided at 1 Hz sampling, and so we used linear interpolation to resample these fields to the native 20 Hz rate of the altimeter measurements. The echoing point was then relocated to the point of closest approach [Roemer *et al.*, 2007] within the SAR beam footprint using a DEM derived from 7 years of CryoSat-2 data [Slater *et al.*, 2017]. Relocated points falling outside of the ~ 0.3 by 18 km SAR beam footprint, together with relocated elevations that deviated by more than 100 meters from the DEM, were removed.

To evaluate the accuracy of the derived Sentinel-3 ice sheet elevation measurements, we used independent elevation data acquired by the Airborne Topographic Mapper (ATM) and Riegl Laser Altimeter (RLA) instruments carried on Operation IceBridge campaigns flown between 2009 and 2016. At our two inland study sites we used ATM measurements, which provide high quality surface elevation measurements with an along-track sampling of 50 meters, and an 80-meter across-track platelet at nadir. These measurements have been estimated to offer a vertical accuracy and precision of 7 cm and 3 cm, respectively [Martin *et al.*, 2012]. At our two coastal sites, where ATM measurements have not been acquired, we used RLA acquisitions. This instrument has a smaller ground footprint of 25 m along track by 1 meter across track, and a slightly larger reported accuracy of 12 cm [Blankenship *et al.*, 2013].



To compute elevation differences between our Sentinel-3 and IceBridge validation datasets, we identified IceBridge records within a 100-meter search radius of each satellite measurement. Where multiple IceBridge records existed within the search radius, we selected the closest measurement. We identified and removed anomalous IceBridge elevation records that deviated by more than 100 meters from an independent DEM [Slater *et al.*, 2017]. We then corrected for elevation differences arising from the spatial and temporal separation of the satellite and airborne measurements, using the difference in DEM elevations at the measurement locations and an estimate of the local rate of elevation change [McMillan *et al.*, 2014], respectively. Finally we computed the difference in elevation between each IceBridge-Sentinel-3 measurement pair and so generated a set of statistics for each study site (Table 2). Because the differences, particularly at coastal sites, were not normally distributed, we principally use the median and median absolute deviation (MAD) from the median as measures of the bias and dispersion, respectively. Additional statistical measures are, however, included within Table 2.

4. Delay-Doppler Measurement Precision

We firstly investigated the shot-to-shot precision of the novel SRAL instrument, together with the stability of measurements through time. For this purpose we focused on the ice surface above subglacial Lake Vostok, which provides a stable and low-slope surface that is well suited to this task [Shuman *et al.*, 2006; Richter *et al.*, 2014; Schröder *et al.*, 2017]. Between December 2016 and December 2017, the satellite made 14 passes over the lake, and so, focusing on two ground tracks that crossed the flat ($< 0.01^\circ$) central portion of the lake (Figure 2), we assessed the repeatability of these measurements in space and time. For each ground track, we extracted the 14 elevation profiles. We then computed (1) the mean elevation profile, (2) the residual elevations from the mean profile, and (3) the standard deviation of all elevation measurements within 400 m intervals along-track (Figure 2). Together these provide an assessment of the instrument shot-to-shot precision over ice sheet surfaces under the influence of minimal topography, and also the repeatability of measurements through time. We find that, over the first year of routine operations, the SAR altimeter has operated with sub-decimeter precision. On average, the 14-cycle standard deviation along both tracks was 7 cm, and rarely fell outside of the range of 5-10 cm along the entirety of the track segment analysed (Figure 2).

25

5. Delay-Doppler Elevation Accuracy

To establish an independent evaluation of the accuracy of the Sentinel-3 altimeter over ice sheets, we compared data from the first year of routine operations to Operation IceBridge airborne elevation measurements. At the inland sites of Lake Vostok and Dome C, we find very good agreement between the Sentinel-3 and airborne datasets (Figure 3). At Lake Vostok, the median bias between the two datasets is 2 cm, and the MAD dispersion is 13 cm. At Dome C, the bias and dispersion are

30



21 cm and 6 cm, respectively. Across both sites, more than 97 % of validation points yielded an elevation difference of less than 50 cm (Table 2), and 70 % (Vostok) and 49 % (Dome C) were less than 20 cm. Given the different operating frequencies, footprint sizes and time periods of the satellite and airborne acquisitions, the low bias at these dry, inland sites is particularly encouraging, because it suggests that the SAR waveform leading edge is not overly sensitive to radar penetration and the induced subsurface scattering from within the near surface snowpack. Equally important for many glaciological applications is the low dispersion of differences, which is typically of the order of 10 cm in magnitude (Table 2). This is consistent with our previous analysis of the instrument precision above Lake Vostok, and suggests that at these relatively low slope inland sites, uncorrelated sources of error, for example due to imprecision of the retracker, radar speckle, the slope correction, or sub-annual variations in snowpack characteristics, have not significantly affected the SAR altimeter elevation measurements.

At the coastal sites of Dronning Maud Land and Wilkes Land the differences between the Sentinel-3 and airborne datasets are, as expected, more widely dispersed than at our inland study locations (Figure 4). The more rugged coastal topographic relief can produce complex waveforms, as energy is often returned from several distinct surfaces within the illuminated beam footprint. These factors represent well-established challenges for radar altimetry, both for retracking algorithms and for the procedure of correctly locating the on-the-ground origin of the derived elevation measurement. SAR altimetry, due to its smaller ground footprint, has the potential to be less affected by these topographic influences, and indeed we find that the overall median biases relative to IceBridge remain small, namely 0.03 m and 0.12 m at Dronning Maud Land and Wilkes Land, respectively. The magnitude of these biases is comparable to those found at our inland sites, suggesting that for a metric that is robust to outliers, no systematic bias is introduced as large scale topographic complexity increases.

For our coastal sites, the dispersion of the elevation differences relative to IceBridge is larger, as demonstrated by the MAD values of 0.30 m and 0.74 m at Dronning Maud Land and Wilkes Land, respectively (Table 2). Nonetheless, these first results demonstrate that even in these challenging regions, the MAD precision of SAR elevation measurements is well below 1 meter. At these sites, we find that ~ 60-85 % of the validated satellite elevation measurements are within 1 meter of their airborne counterpart, and 92-98 % are within 10 meters (Table 2). As is evident from these statistics, and also the standard deviation of the differences (Table 2), there are a small number of outlying measurements that exhibit larger deviations from the airborne validation datasets. Given the focus of this study we have not removed these outliers, although we note that for many future glaciological applications it may be beneficial to do so.

Considering the validation statistics across all four study sites, the pattern of increasing dispersion of elevation differences at coastal locations is consistent with our understanding that measurement precision degrades with increasing topographic complexity. In contrast, it is perhaps more unexpected that the largest median bias, of 20 cm, would be found at the Dome C site. While validation data is limited at this site, and so the anomaly may be related to the specific airborne campaign



conducted in this region, it nonetheless warranted further investigation. We therefore used the IceBridge data to assess the fine scale topography at this site, and to compare it to the ice surface above Lake Vostok, which has similar large scale topographic characteristics but where negligible bias is evident (Table 2). Specifically, we removed the long wavelength signal from each elevation profile using a quadratic fit and plotted the elevation residuals from this model fit (Figure 5).

5 Although the large scale topographic regime at both sites is broadly smooth and flat, these airborne flightlines show that Dome C presents a much rougher surface at 100-500 m length scales, with amplitudes typically ranging from ~ 5-30 cm. In comparison, the amplitude of oscillations at Lake Vostok is typically 1-5 cm. It is therefore possible that part of the larger bias at Dome C can be explained by the rougher surface, and the tendency of the satellite altimeter, given its larger footprint, to be more influenced by the local topographic peaks than the airborne instrument. We also note that it could be possible to

10 tune our processing to reduce the bias at this site, by selecting a higher retracking point on the waveform leading edge that is closer to the theoretical mean return from a surface with these roughness characteristics. However, we reiterate that our philosophy here is to use a conservative retracking threshold that is likely to deliver robust and stable results across all types of topographic regimes, and one that is therefore well-suited to delivering reliable continent-wide estimates of surface elevation change through time.

15

6. Ice Sheet elevation change from Delay-Doppler Altimetry

Our analysis has provided the first comprehensive assessment of measurements of ice sheet elevation derived using Sentinel-3 Delay-Doppler (SAR mode) altimetry, and an initial demonstration of their accuracy and precision across a range of topographic regimes. Within a wider geophysical context, one of the principle uses of altimetry data is to determine changes in ice sheet elevation over time [Zwally *et al.*, 2005; Shepherd and Wingham, 2007; Flament and Rémy, 2012; Shepherd *et al.*, 2012]. Although the time period of Sentinel-3 acquisitions to date is short for detailed glaciological interpretation of any signals, it is nonetheless of interest to establish (1) the extent to which the system has provided a stable measurement platform in time, and (2) whether the precision and accuracy of these novel SAR measurements is sufficient to be able to resolve known signals of glaciological change. As a preliminary investigation of these questions, we therefore used a

25 modified model-fit method [McMillan *et al.*, 2014, 2016] applied to all available Sentinel-3 data acquired to date (up to cycle 27) to explore the potential of these novel data for mapping elevation changes of the Antarctic Ice Sheet. In summary, we firstly removed an *a priori* estimate of elevation from each measurement using an auxiliary DEM [Slater *et al.*, 2017], rejecting records that deviated by more than 50 m from the same DEM. We then used the resulting elevation residuals to simultaneously solve for linear spatial and temporal rates of elevation change on a 5 x 5 km grid. We rejected grid cells

30 where the model produced a poor or geophysically unrealistic fit to the data, defined as where the root-mean-square of the observed-minus-model residuals exceeded 2 meters, the absolute rate of elevation change exceeded 10 m yr^{-1} , the derived surface slope exceeded 5° , or where less than 20 measurements constrained the model fit.



Using this method, we determined an estimate of the rate of ice sheet elevation change across a total area of 5 061 700 km², constituting 42.3 % of the ice sheet (Figure 6). Across large parts of the slow-flowing ice sheet interior, the derived rates of elevation change are low. This agrees with numerous recent studies [*Flament and Rémy*, 2012; *Helm et al.*, 2014; *McMillan et al.*, 2014], and provides an early indication that the Sentinel-3 instrument and orbital configuration is suitable for mapping changes across the low relief ice sheet interior. Across the margins of the ice sheet, even over this short time period, there is evidence that Delay-Doppler altimetry is able to map the higher, dynamically-driven, rates of elevation change in these topographically more complex regions. Rates of surface lowering of ~1-5 m yr⁻¹ are evident across the fast-flowing ice streams draining into the Amundsen Sea Sector of West Antarctica, close to the grounding lines of the Pine Island, Thwaites, and Smith Glaciers. In comparison to inland regions, the coverage is generally poorer across the steeper ice margin regions and the more mountainous terrain of the Antarctic Peninsula. This is expected given the lower precision of elevation measurements in these locations, the wider track spacing, and the short time period over which the trends are being computed. Additionally, it is important to note that the current approach to performing the SAR multi-looking within the Level-1B processing chain of the ground segment is not fully optimized for these challenging ice regions. Further refinements to this processing step, namely to adjust the windowing during the Doppler beam stacking to account for large variations in the satellite tracker range, are currently being implemented, and are expected to deliver future improvements in data retrieval in these regions. Based upon this preliminary assessment, however, there is good reason to expect that Sentinel-3 Delay-Doppler altimetry will prove to be an effective tool for mapping ice sheet elevation change.

20 7. Conclusions

We have undertaken a first assessment of the utility of Sentinel-3 Delay-Doppler (SAR mode) altimetry for measuring ice sheet elevation and elevation change using the standard ESA Level-1b product and our own dedicated Level-2 processing chain. Analysis of repeated acquisitions over the Lake Vostok validation site indicates that, over the first year of routine operations, the instrument has operated with sub-decimeter precision. Through validation with airborne campaigns, we find small median biases in elevation, typically of the order 1-10 cm, at both inland and coastal sites. The dispersion of elevation residuals, measured with respect to the validation data, is of the order of 10 cm at inland sites, increasing to ~30-80 cm at coastal sites with more complex topography. This is likely to reflect the main challenges associated with processing radar altimetry data in complex ice margin regions, namely (1) reliable retracking of multippeak waveforms that arise when multiple distinct surface reflections are captured within the receive window, and (2) accurately establishing the location of the echoing point within the SAR beam footprint. These represent principle avenues of future research within the developing field of ice sheet Delay-Doppler altimetry. Nonetheless, the sub-meter accuracy achieved in even these complex ice margin regions is encouraging, and expected to improve further as refinements are made to the operational ground segment



processing. Finally, we have shown the capability of Sentinel-3, albeit with the relatively short record of data currently available, to resolve the known signals of elevation change that currently dominate Antarctica's contribution to sea level rise. Together, our analysis demonstrates the early promise of Sentinel-3 SAR altimetry as a platform for long-term, operational monitoring of Earth's ice sheets.

5

8. Data Availability

The Sentinel-3 altimetry data used in this study are freely available through the Copernicus Open Access Hub (<https://scihub.copernicus.eu/dhus/#/home>). The IceBridge airborne altimetry data used in this study are freely available from the US National Snow and Ice Data Center (<https://nsidc.org/>). The CryoSat-2 DEM used in this study is freely distributed by the UK NERC Centre for Polar Observation and Modelling (<http://www.cpom.ucl.ac.uk/csopr/icesheets2>).

10

9. Author Contribution

MM designed the experiments. MM and AM processed and analysed the data. MM prepared the manuscript with contributions from AS, MR, AA and JB, and all authors reviewed the manuscript. The authors declare that they have no conflict of interest.

15

10. Acknowledgements

This work was supported by the UK NERC Centre for Polar Observation and Modelling, the European Space Agency contract *SEOM – Sentinel-3 Performance Improvements for ICE sheets* (contract number 4000115201/15/1-BG), and the *Sentinel-3 Mission Performance Centre*.

20

References

- Bamber, J. L., and R. A. Bindschadler (1997), An improved elevation dataset for climate and ice-sheet modelling: validation with satellite imagery, edited by J. E. Walsh, *Ann. Glaciol.*, 25, 438–444.
- 25 Bamber, J. L., J. L. Gomez-Dans, and J. A. Griggs (2009), A new 1 km digital elevation model of the Antarctic derived from combined satellite radar and laser data - Part 1: Data and methods, *Cryosph.*, 3(1), 101–111.
- Blankenship, D. D., S. D. Kempf, D. A. Young, J. L. Roberts, T. van Ommen, R. Forsberg, M. J. Siegert, S. J. Palmer, and J.



- A. Dowdeswell (2013), IceBridge Riegl Laser Altimeter L2 Geolocated Surface Elevation Triplets, Version 1, Boulder, Color. USA. NASA Natl. Snow Ice Data Cent. Distrib. Act. Arch. Cent., doi:<https://doi.org/10.5067/JV9DENETK13E>.
- Bogning, S. et al. (2018), Monitoring Water Levels and Discharges Using Radar Altimetry in an Ungauged River Basin: The
5 Case of the Ogooué, *Remote Sens.*, 10(3), 350, doi:10.3390/rs10020350.
- Bonnefond, P. et al. (2018), Calibrating the SAR SSH of Sentinel-3A and CryoSat-2 over the Corsica Facilities, *Remote Sens.*, 10(2), 92, doi:10.3390/rs10010092.
- Chelton, D. B., E. J. Walsh, and J. L. MacArthur (1989), Pulse Compression and Sea Level Tracking in Satellite Altimetry, *J. Atmos. Ocean. Technol.*, 6(3), 407–438, doi:10.1175/1520-0426.
- 10 Davis, C., and A. Ferguson (2004), Elevation change of the Antarctic ice sheet, 1995–2000, from ERS-2 satellite radar altimetry, *IEEE Trans. Geosci. Remote Sens.*, 42(11), 2437–2445, doi:10.1109/TGRS.2004.836789.
- Davis, C. H., Y. H. Li, J. R. McConnell, M. M. Frey, and E. Hanna (2005), Snowfall-driven growth in East Antarctic ice sheet mitigates recent sea-level rise, *Science (80-.)*, 308(5730), 1898–1901, doi:10.1126/science.1110662.
- Donlon, C. et al. (2014), The Global Monitoring for Environment and Security (GMES) Sentinel-3 mission, *Remote Sens. Environ.*, 120(2012), 37–57, doi:10.1016/j.rse.2011.07.024.
- 15 Flament, T., and F. Rémy (2012), Dynamic thinning of Antarctic glaciers from along-track repeat radar altimetry, *J. Glaciol.*, 58(211), 830–840, doi:10.3189/2012JoG11J118.
- Gray, L., D. Burgess, L. Copland, M. N. Demuth, T. Dunse, K. Langley, and T. V. Schuler (2015), CryoSat-2 delivers monthly and inter-annual surface elevation change for Arctic ice caps, *Cryosph. Discuss.*, 9(3), 2821–2865,
20 doi:10.5194/tcd-9-2821-2015.
- Haran, T., J. Bohlander, T. Scambos, T. Painter, and M. Fahnestock (2006), MODIS mosaic of Antarctica (MOA) image map,
- Helm, V., a. Humbert, and H. Miller (2014), Elevation and elevation change of Greenland and Antarctica derived from CryoSat-2, *Cryosph.*, 8(4), 1539–1559, doi:10.5194/tc-8-1539-2014.
- 25 Heslop, E. E., A. Sánchez-Román, A. Pascual, D. Rodríguez, K. A. Reeve, Y. Faugère, and M. Raynal (2017), Sentinel-3A Views Ocean Variability More Accurately at Finer Resolution, *Geophys. Res. Lett.*, 44(24), 12,367–12,374, doi:10.1002/2017GL076244.
- Hurkmans, R. T. W. L., J. L. Bamber, C. H. Davis, I. R. Joughin, K. S. Khvorostovsky, B. S. Smith, and N. Schoen (2014), Time-evolving mass loss of the Greenland ice sheet from satellite altimetry, *Cryosph.*, 8, 1725–1740, doi:10.5194/tcd-
30 8-1057-2014.
- Johannessen, O. M., K. Khvorostovsky, M. W. Miles, and L. P. Bobylev (2005), Recent ice-sheet growth in the interior of Greenland., *Science (80-.)*, 310(5750), 1013–6, doi:10.1126/science.1115356.
- Martin, C. F., W. B. Krabill, S. S. Manizade, R. L. Russell, J. G. Sonntag, R. N. Swift, and J. K. Yungel (2012), Airborne Topographic Mapper Calibration Procedures and Accuracy Assessment, *NASA Tech. Rep. NASA/TM/20132012-*



- 215891, *Goddard Sp. Flight Center, Greenbelt, Maryl.* 20771. Available online
<http://ntrs.nasa.gov/archive/nasa/casi.ntrs.nasa.gov/20120008479.pdf>.
- McMillan, M., A. Shepherd, A. Sundal, K. Briggs, A. Muir, A. Ridout, A. Hogg, and D. Wingham (2014), Increased ice losses from Antarctica detected by CryoSat-2, *Geophys. Res. Lett.*, *41*(11), 1–7, doi:10.1002/2014GL060111.
- 5 McMillan, M. et al. (2016), A high-resolution record of Greenland mass balance, *Geophys. Res. Lett.*, *43*(13), doi:10.1002/2016GL069666.
- McMillan, M., A. Shepherd, A. Muir, J. Gaudelli, A. E. Hogg, and R. Cullen (2017), Assessment of CryoSat-2 interferometric and non-interferometric SAR altimetry over ice sheets, *Adv. Sp. Res.*, doi:10.1016/j.asr.2017.11.036.
- Price, S. F., A. J. Payne, I. M. Howat, and B. E. Smith (2011), Committed sea-level rise for the next century from Greenland ice sheet dynamics during the past decade., *Proc. Natl. Acad. Sci. U. S. A.*, *108*(22), 8978–83, doi:10.1073/pnas.1017313108.
- 10 Raney, K. (1998), The delay/doppler radar altimeter, *IEEE Trans. Geosci. Remote Sens.*, *36*(5), 1578–1588, doi:10.1109/36.718861.
- Remy, F., P. Mazzega, S. Houry, C. Brossier, and J. F. Minster (1989), Mapping of the Topography of Continental Ice by Inversion of Satellite-Altitude Data, *J. Glaciol.*, *35*(119), 98–107, doi:10.3189/002214389793701419.
- 15 Richter, A. et al. (2014), Height changes over subglacial Lake Vostok, East Antarctica: Insights from GNSS observations, *J. Geophys. Res.*, *119*, doi:10.1002/2014JF003228. Received.
- Roemer, S., B. Legrésy, M. Horwath, and R. Dietrich (2007), Refined analysis of radar altimetry data applied to the region of the subglacial Lake Vostok/Antarctica, *Remote Sens. Environ.*, *106*(3), 269–284, doi:10.1016/j.rse.2006.02.026.
- 20 Schröder, L. et al. (2017), Validation of satellite altimetry by kinematic GNSS in central East Antarctica, *Cryosph.*, *11*(3), 1111–1130, doi:10.5194/tc-11-1111-2017.
- Shepherd, A., and D. Wingham (2007), Recent sea-level contributions of the Antarctic and Greenland ice sheets, *Science (80-)*, *315*(5818), 1529–1532.
- Shepherd, A., D. Wingham, and E. Rignot (2004), Warm ocean is eroding West Antarctic Ice Sheet, *Geophys. Res. Lett.*, *31*, L23402, doi:L23402 10.1029/2004gl021106.
- 25 Shepherd, A. et al. (2012), A reconciled estimate of ice-sheet mass balance, *Science (80-)*, *338*(6111), doi:10.1126/science.1228102.
- Shuman, C. A., H. J. Zwally, B. E. Schutz, A. C. Brenner, J. P. DiMarzio, V. P. Suchdeo, and H. A. Fricker (2006), ICESat Antarctic elevation data: Preliminary precision and accuracy assessment, *Geophys. Res. Lett.*, *33*(7), L07501, doi:10.1029/2005GL025227.
- 30 Slater, T., A. Shepherd, M. McMillan, A. Muir, L. Gilbert, A. E. Hogg, H. Konrad, and T. Parrinello (2017), A new Digital Elevation Model of Antarctica derived from CryoSat-2 altimetry, *Cryosph. Discuss.*, 1–26, doi:10.5194/tc-2017-223.
- Sørensen, L. S., S. B. Simonsen, R. Meister, R. Forsberg, J. F. Levensen, and T. Flament (2015), Envisat-derived elevation changes of the Greenland ice sheet, and a comparison with ICESat results in the accumulation area, *Remote Sens.*



- Environ.*, 160, 56–62, doi:10.1016/j.rse.2014.12.022.
- Wingham, D., D. Wallis, and A. Shepherd (2009), Spatial and temporal evolution of Pine Island Glacier thinning, 1995–2006, *Geophys. Res. Lett.*, 36, L17501, doi:L17501 10.1029/2009gl039126.
- Wingham, D. J., C. G. Rapley, and H. D. Griffiths (1986), New techniques in satellite altimeter tracking systems, *Proc. IGARSS Symp. Zurich, 8–11 Sept. 1986, SP-254*, 1339–1344.
- 5
- Wingham, D. J. et al. (2006a), CryoSat: A mission to determine the fluctuations in Earth’s land and marine ice fields, in *NATURAL HAZARDS AND OCEANOGRAPHIC PROCESSES FROM SATELLITE DATA*, vol. 37, edited by M. Singh, RP and Shea, pp. 841–871, ELSEVIER SCIENCE LTD.
- Wingham, D. J., A. Shepherd, A. Muir, and G. J. Marshall (2006b), Mass balance of the Antarctic ice sheet, *Philos. Trans. R. Soc. A-MATHEMATICAL Phys. Eng. Sci.*, 364(1844), 1627–1635, doi:10.1098/rsta.2006.1792.
- 10
- Zwally, H. J., M. B. Giovinetto, J. Li, H. G. Cornejo, M. A. Beckley, A. C. Brenner, J. L. Saba, and D. Yi (2005), Mass changes of the Greenland and Antarctic ice sheets and shelves and contributions to sea-level rise: 1992 – 2002, *J. Glaciol.*, 51(175), 1992–2002.
- Zwally, H. J. et al. (2011), Greenland ice sheet mass balance: distribution of increased mass loss with climate warming; 2003–07 versus 1992–2002, *J. Glaciol.*, 57(201), 88–102, doi:10.3189/002214311795306682.
- 15

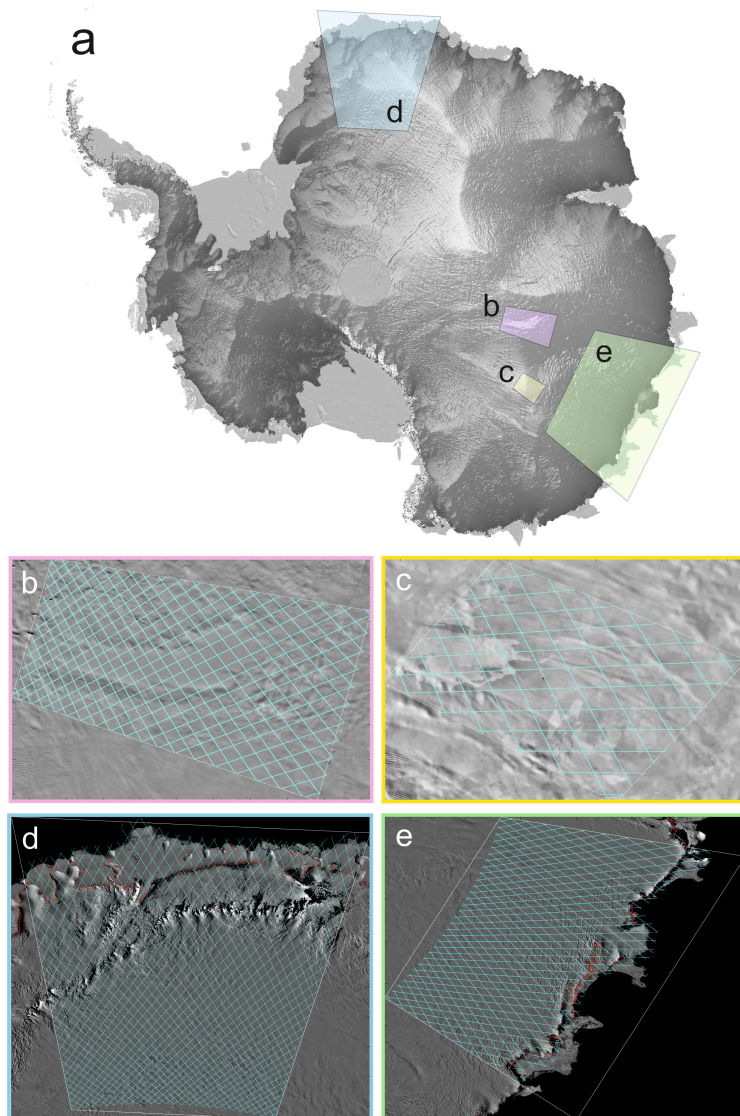


Figure 1. a. Overview of the Lake Vostok (b), Dome C (c), Dronning Maud Land (d) and Wilkes Land (e) study sites. The background image in panel a is a surface DEM [Slater *et al.*, 2017] overlaid upon the MODIS Mosaic of Antarctica (MOA) [Haran *et al.*, 2006]. Panels b-e show the Sentinel-3 ground tracks (turquoise) at each study site, overlaid upon MOA.

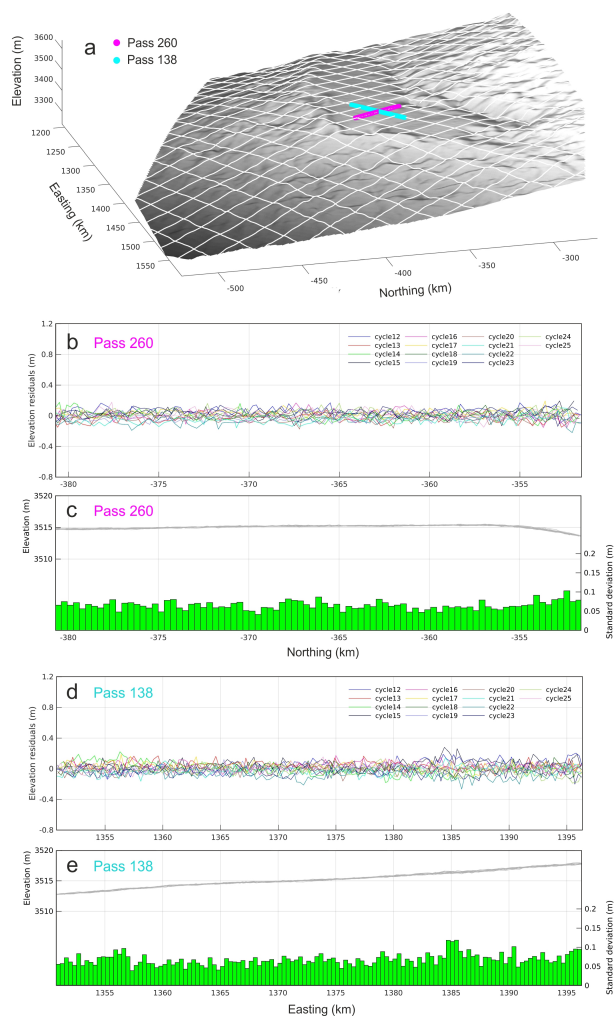


Figure 2. Assessment of instrument precision at the Lake Vostok site in East Antarctica. **a.** The location of the two ground tracks crossing the center of the lake (Pass 138, cyan; Pass 260, magenta), plotted on a surface DEM [Slater *et al.*, 2017], with other passes shown in white. For each pass, 14 cycles were accumulated between Dec. 2016 and Dec 2017. Panels **b** and **d** show the residuals from the mean elevation of all cycles. Panels **c** and **e** show the elevations along each pass (grey), together with the standard deviations of all measurements acquired at 400 m intervals (green bars).

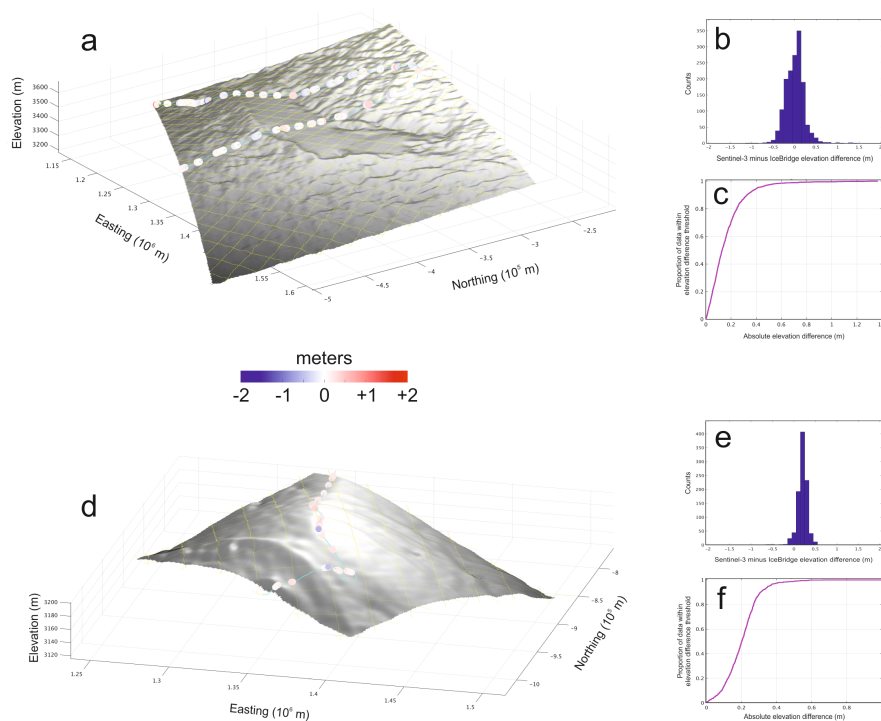


Figure 3. Assessment of the accuracy of Sentinel-3A elevation measurements at the inland Lake Vostok (a-c) and Dome C (d-f) sites in East Antarctica. a,d. Elevation differences between Sentinel-3 and IceBridge. Sentinel-3 and IceBridge tracks are shown as thin white and turquoise tracks lines, respectively, and the background image is constructed from a CryoSat-2 DEM [Slater *et al.*, 2017]. b,e. Distribution of Sentinel-3 – IceBridge elevation differences at the Lake Vostok (b) and Dome C (e) sites. c,f. Cumulative distribution of the absolute Sentinel-3 – IceBridge elevation differences at the Lake Vostok (c) and Dome C (f) sites.

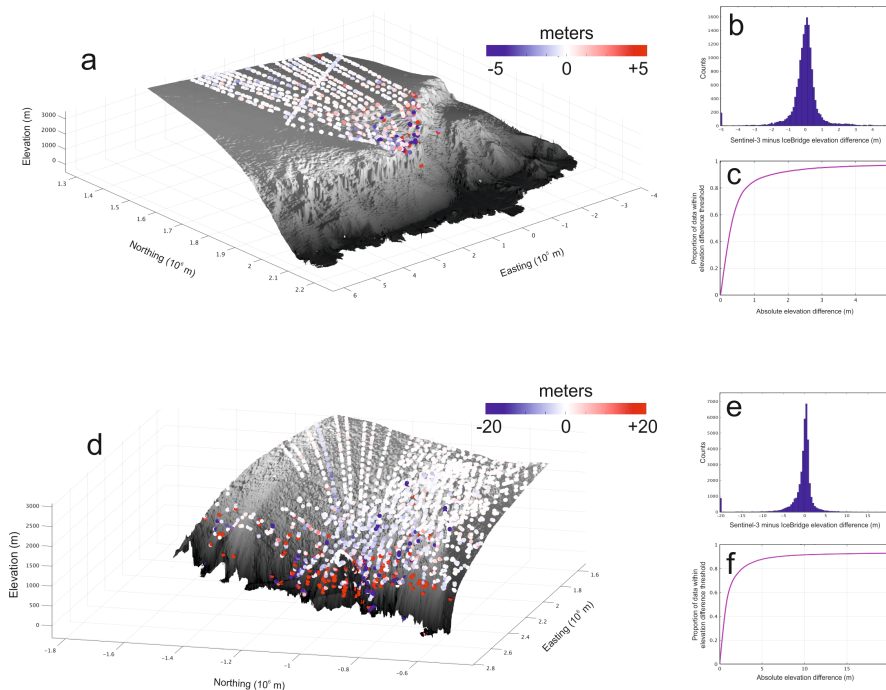


Figure 4. Assessment of the accuracy of Sentinel-3A elevation measurements at the coastal Dronning Maud Land (a-c) and Wilkes Land (d-f) sites in East Antarctica. a,d. Elevation differences between Sentinel-3 and IceBridge. The background image is constructed from a CryoSat-2 DEM [Slater *et al.*, 2017] and the colour scales differ for the two sites. b,e. Distribution of Sentinel-3 – IceBridge elevation differences at the Dronning Maud Land (b) and Wilkes Land (e) sites. c,f. Cumulative distribution of the absolute Sentinel-3 – IceBridge elevation differences at the Dronning Maud Land (c) and Wilkes Land (f) sites.

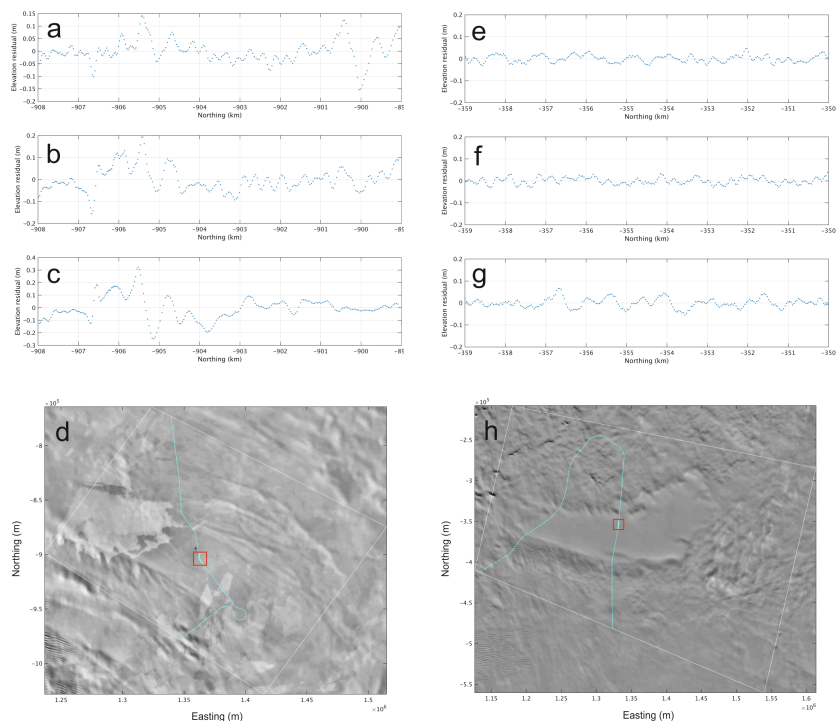


Figure 5. Comparison of 100 metre scale surface roughness at Dome C (a-d) and Lake Vostok (e-h). Panels a-c and e-g show profiles of elevation residuals acquired by the ATM airborne instrument at the locations marked by the red boxes in panels d and h, respectively. Residuals are computed by removing a quadratic trend from each elevation profile. In panels d and h, the airborne ground track is shown in turquoise, the bounds of the study area in white, and the background image is from the MODIS Mosaic of Antarctica (MOA) [Haran *et al.*, 2006].

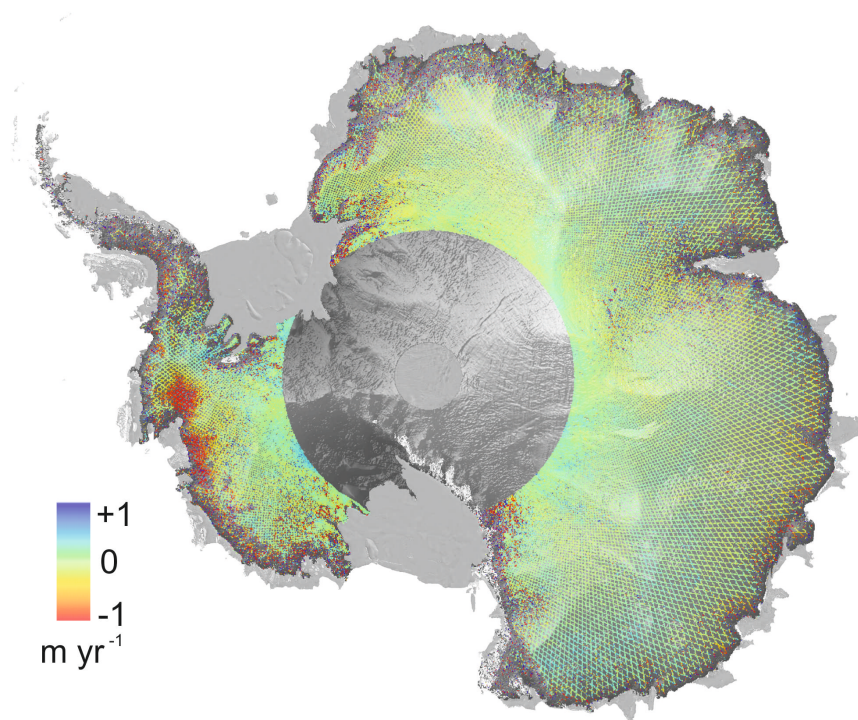


Figure 6. Rates of Antarctic surface elevation change derived from Sentinel-3A Delay-Doppler altimetry acquired between May 2016 and February 2018. The background image is a shaded relief derived from a DEM [Slater *et al.*, 2017], overlaid upon the MODIS Mosaic of Antarctica (MOA) [Haran *et al.*, 2006].



Table 1. Summary of Sentinel-3 orbit characteristics and the primary altimeter payload.

Sentinel-3A launch date	16 th Feb. 2016
Sentinel-3B launch date	25 th Apr. 2018
Orbital Inclination	98.65°
Orbital altitude	~ 830 km
Repeat period	27 days
SRAL Central Frequency	13.575 GHz
Antenna footprint diameter	~ 18 km
Along-track measurement interval	~ 330 m
Along-track resolution	~ 300 m
Across-track resolution	~ 1600-3000 m



Table 2. Sentinel-3A validation statistics based upon comparison to IceBridge airborne altimetry at the four study sites.

	Vostok	Dome C	Dronning Maud Land	Wilkes Land
Number of measurements	1528	969	16462	40400
Median elevation difference (m)	0.02	0.21	0.03	0.12
Mean elevation difference (m)	0.003	0.20	0.42	1.43
Median absolute deviation of elevation differences (m)	0.13	0.06	0.30	0.74
Standard deviation of elevation differences (m)	0.22	0.12	7.30	14.99
RMS of elevation differences (m)	0.22	0.23	7.31	15.06
% points within 0.5 meter of IceBridge elevation	97.3	98.9	68.5	35.0
% points within 1 meter of IceBridge elevation	99.5	99.9	85.0	58.8
% points within 10 meters of IceBridge elevation	100	100	98.1	91.6